A Quantum Chemical Exploration of the Horner−Wadsworth−Emmons Reaction

Peter Brandt,*[,†] Per-Ola Norrby,[‡] Ivar Martin,[§] and Tobias Rein*[,†,∥]

Department of Chemistry, Organic Chemistry, Royal Institute of Technology, S-100 44 Stockholm, Sweden, Department of Medicinal Chemistry, Royal Danish School of Pharmacy, Universitetsparken 2, DK-2100 Copenhagen, Denmark, Department of Bioorganic Chemistry, Institute of Chemistry, Akadeemia tee 15, EE 0026 Tallinn, Estonia, and Department of Organic Chemistry, Technical University of Denmark, DK-2800, Lyngby, Denmark

Received October 27, 1997

The mechanism of the Horner−Wadsworth−Emmons (HWE) reaction has been investigated using high level quantum mechanical calculations on a realistic model system. The solvation contribution has been evaluated using the PCM/DIR method. In the free, anionic system, the rate-determining step was found to be the ring closure of an oxyanion to an oxaphosphetane. Solvation was found to have a drastic influence on the reaction path. In most solvated systems, the bimolecular formation of the oxyanion intermediate may be rate limiting. Previously postulated isomerization side paths were investigated. Several effects that could rationalize experimentally observed trends for (*E*)/(*Z*)-selectivities have been identified.

Introduction

The Wittig reaction and its variants are of key importance to the practicing synthetic organic chemist.[1] Both the scope[1b,c] and the mechanism[1a,c,2] of the parent Wittig reaction, in particular, have been extensively studied, and considerable effort has been devoted also to reactions involving phosphonate reagents[1b−f,3] [commonly called Horner−Wadsworth−Emmons (HWE) reactions]; nevertheless, important mechanistic details still remain to be elucidated. In particular, it is notable that higher level computational studies related to the HWE reaction mechanism have begun to emerge only very recently.[3]

Possible mechanistic alternatives for the HWE reaction are illustrated in Scheme 1. Diastereomeric oxyanions[4] **3** and oxaphosphetanes[5] **4** are generally believed to be either intermediates or transition states on the reaction pathway, and the involvement of a stable ring-cleaved enolate **5** has also been suggested.[6]

Intermediates **3**−**5** contain additional stereocenters which are not present in either reactants or products, but nonetheless the configurations at these centers determine the stereochemistry of the final product. If either intermediate is long-lived enough, crossover between diastereomeric pathways could plausibly take place via tautomeric proton shifts[4b,7] in **3** or **4**, or via C−C bond rotation in **5**.[6] Furthermore, the stereochemistry of the reaction will be affected by the potential reversibility of the initial addition step.[4a,b,8] Commonly, the stereoselectivity in Wittig-type reactions is rationalized by invoking transition state models such as those depicted in Figure 1.

The chelated TS1 can be of importance when coordinating metal ions are present. In the absence of stabilization by coordination (as in the model system of interest in the present work), the strong electrostatic repulsion between the oxygens would be expected to favor other rotamers of *gauche*-g-TS1 (Figure 1).

With aldehydes other than formaldehyde, the carbon substituent preferably occupies the least hindered site in each transition state. In *anti*-TS1, the pro-(*E*) position is gauche to two large groups and therefore expected to be disfavored. The same is true for the pro-(*Z*) position in *gauche*-a-TS1. The third possible TS1 (*gauche*-g-TS1)

† Royal Institute of Technology.
‡ Royal Danish School of Pharmacy.
§ Institute of Chemistry.
∥ Technical University of Denmark. e-mail: oktr@pop.dtu.dk.

(1) For reviews, see: (a) Vedejs, E.; Peterson, M. J. *Topics in Stereochemistry* **1994**, *21*, 1−157. (b) Kelly, S. E. In *Comprehensive Organic Synthesis*; Trost, B. M., Fleming, I., Eds.; Pergamon Press: Oxford, 1991; Vol. 1, pp 730−817. (c) Maryanoff, B. E.; Reitz, A. B. *Chem. Rev. (Washington, D.C.)* **1989**, *89*, 863−927. (d) Walker, B. J. In *Organophosphorus Reagents in Organic Synthesis*; Cadogan, J. I. G., Ed.; Academic Press: New York, 1979; pp 155−205. (e) Wadsworth, W. S., Jr. *Org. React.* **1977**, *25*, 73−253. (f) Boutagy, J.; Thomas, R. *Chem. Rev. (Washington, D.C.)* **1974**, *74*, 87−99.

(2) Recent contributions: (a) Yamataka, H.; Takatsuka, T.; Hanafusa, T. *J. Org. Chem.* **1996**, *61*, 722−726. (b) Takeuchi, K.; Paschal, J. W.; Loncharich, R. J. *J. Org. Chem.* **1995**, *60*, 156−168. (c) Naito, T.; Nagase, S.; Yamataka, H. *J. Am. Chem. Soc.* **1994**, *116*, 10080−10088. (d) Geletneky, C.; Försterling, F.-H.; Bock, W.; Berger, S. *Chem. Ber.* **1993**, *126*, 2397−2401.

(3) (a) Koch, R.; Anders, E. *J. Org. Chem.* **1995**, *60*, 5861−5866. (b) Zarges, W.; Marsch, M.; Harms, K.; Haller, F.; Frenking, G.; Boche, G. *Chem. Ber.* **1991**, *124*, 861−866. See also: (c) Kranz, M.; Denmark, S. E. *J. Org. Chem.* **1995**, *60*, 5867−5877, and references therein. (d) Cramer, C. J.; Denmark, S. E.; Miller, P. C.; Dorow, R. L.; Swiss, K. A.; Wilson, S. R. *J. Am. Chem. Soc.* **1994**, *116*, 2437−2447. For an example of modeling of an asymmetric HWE reaction by use of molecular mechanics calculations, see: (e) Narasaka, K.; Hidai, E.; Hayashi, Y.; Gras, J.-L. *J. Chem. Soc., Chem. Commun.* **1993**, 102−104. For a calculational study of the Horner−Wittig reaction, see: (f) Armstrong, D. R.; Barr, D.; Davidson, M. G.; Hutton, G.; O'Brien, P.; Snaith, R.; Warren, S. *J. Organomet. Chem.* **1997**, *529*, 29−33.

(4) (a) Bottin-Strzalko, T.; Seyden-Penne, J. *Bull. Soc. Chim. Fr.* **1984 (II)**, 161−163. (b) Deschamps, B.; Lefèbvre, G.; Seyden-Penne, J. *Tetrahedron* **1972**, *28*, 4209−4222. (c) Durrant, G.; Sutherland, J. K. *J. Chem. Soc., Perkin Trans. 1* **1972**, 2582−2584. (d) Lefèbvre, G.; Seyden-Penne, J. *J. Chem. Soc., Chem. Commun.* **1970**, 1308−1309.

(5) (a) Larsen, R. O.; Aksnes, G. *Phosphorus Sulfur* **1983**, *15*, 229−237. (b) Larsen, R. O.; Aksnes, G. *Phosphorus Sulfur* **1983**, *15*, 219−228. (c) Breuer, E.; Zbaida, S.; Segall, E. *Tetrahedron Lett.* **1979**, 2203−2204.

(6) (a) Bestmann, H. J. *Pure Appl. Chem.* **1979**, *51*, 515−533. (b) Sturtz, G. *Bull. Soc. Chim. Fr.* **1964**, 2349−2357.

(7) Danion, D.; Carrié, R. *Tetrahedron* **1972**, *28*, 4223−4229.

(8) (a) Etemad-Moghadam, G.; Seyden-Penne, J. *Bull. Soc. Chim. Fr.* **1985**, 448−455. (b) Redjal, A.; Seyden-Penne, J. *Tetrahedron Lett.* **1974**, 1733−1736. (c) Bottin-Strzalko, T. *Tetrahedron* **1973**, *29*, 4199−4204.

S0022-3263(97)01973-7 CCC: $15.00
Published on Web 01/27/1998

Scheme 1. Postulated Mechanistic Alternatives for the HWE Reaction. Y = RO, R_2N; Z = Anion-Stabilizing Group (e.g., CO_2R)

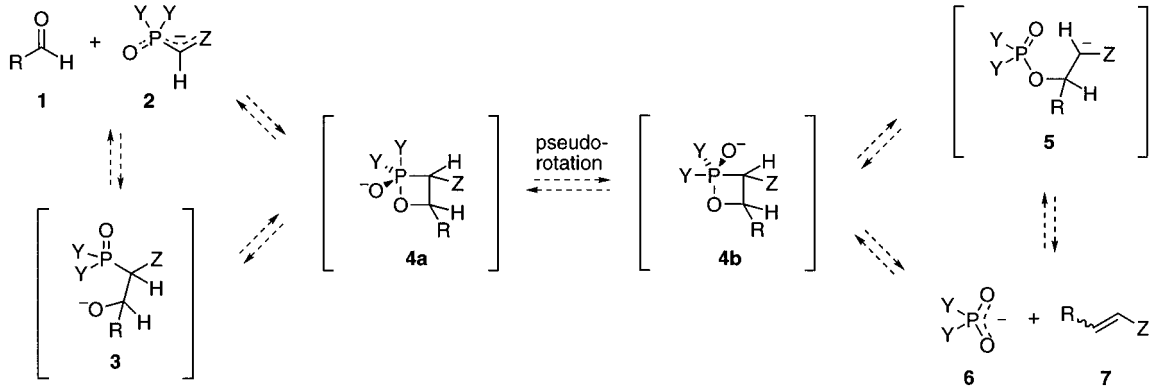

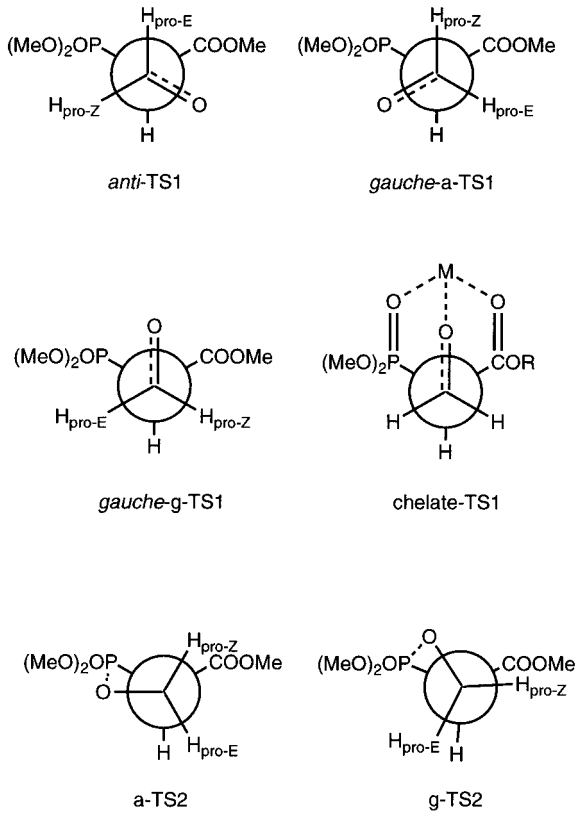

Figure 1. Newman projections of the addition and the ring closure in the model reaction.

is expected to be higher in energy than the other two since the carbonyl oxygen is gauche to two large groups. In TS2, the pro-(*Z*) position is eclipsed with the ester function. On the basis of these arguments, gauche-TS1 and TS2 are expected to favor (*E*)-product, whereas an irreversible addition through *anti*-TS1 can be used to rationalize (*Z*)-selectivity.

In practice, the alkene geometry of the HWE product can often be controlled by an appropriate choice of reagent type[1,9] and reaction conditions.[1,10] This control rests to a large extent on accumulated empirical knowledge. In recent years, asymmetric versions of these reactions have gained increasing interest,[11] and several examples of highly selective reactions have been reported. Further development of this area would benefit strongly from a deeper understanding of the details of the general reaction. With the long-term goal of facilitating rational reagent design, in particular for asymmetric reactions, we have performed a computational study of the HWE reaction. In this paper, we present our results from a high level quantum chemical study of a realistic model system. The major goal of the current study has been to identify the selectivity-determining step(s) of the reaction, but also to give an insight into how variations in reaction conditions can be expected to influence the product distribution, and to furnish raw data for future force field investigations of the HWE reaction.

Methods

The reaction between formaldehyde and trimethyl phosphonoacetate anion (**2**; Y = OMe, Z = CO_2Me) was chosen as a model system. The potential energy surface (PES) of the reactions depicted in Scheme 1 was calculated using the B3LYP hybrid functional[12] together with the 6-31+G* basis set in Gaussian94.[13] The postulated side paths through **8** and **9** (tautomers of **3** and **4**, respectively) were also included. Alternative conformations of all intermediates were investigated exhaustively at lower levels of theory (see Supporting Information). Initial transition state geometries were constructed from low energy forms of both flanking intermediates.

(9) (a) Kokin, K.; Motoyoshiya, J.; Hayashi, S.; Aoyama, H. *Synth. Commun.* **1997**, *27*, 2387−2392. (b) Ando, K. *J. Org. Chem.* **1997**, *62*, 1934−1939, and references therein. (c) Still, W. C.; Gennari, C. *Tetrahedron Lett.* **1983**, *24*, 4405−4408. (d) Larsen, R. O.; Aksnes, G. *Phosphorus Sulfur* **1983**, *16*, 339−344. (e) Nagaoka, H.; Kishi, Y. *Tetrahedron* **1981**, *37*, 3873−3888. (f) Breuer, E.; Bannet, D. M. *Tetrahedron* **1978**, *34*, 997−1002. (g) Breuer, E.; Bannet, D. M. *Tetrahedron Lett.* **1977**, 1141−1144. (h) Deschamps, B.; Lampin, J. P.; Mathey, F.; Seyden-Penne, J. *Tetrahedron Lett.* **1977**, 1137−1140.

(10) (a) Sano, S.; Yokoyama, K.; Fukushima, M.; Yagi, T.; Nagao, Y. *Chem. Commun.* **1997**, 559−560. (b) Thompson, S. K.; Heathcock, C. H. *J. Org. Chem.* **1990**, *55*, 3386-3388. (c) Etemad-Moghadam, G.; Seyden-Penne, J. *Tetrahedron* **1984**, 5153−5166. (d) Deschamps, B.; Lefebvre, G.; Redjal, A.; Seyden-Penne, J. *Tetrahedron* **1973**, *29*, 2437−2444.

(11) For reviews, see: (a) Li, A.-H.; Dai, W.-M.; Aggarwal, V. K. *Chem. Rev. (Washington, D.C.)* **1997**, *97*, 2341−2372. (b) Rein, T.; Reiser, O. *Acta Chem. Scand.* **1996**, *50*, 369−379. Recent examples: (c) Kumamoto, T.; Koga, K. *Chem. Pharm. Bull.* **1997**, *45*, 753−755. (d) Dai, W.-M.; Wu, J.; Huang, X. *Tetrahedron: Asymmetry* **1997**, *8*, 1979−1982. (e) Kreuder, R.; Rein, T.; Reiser, O. *Tetrahedron Lett.* **1997**, *38*, 9035−9038. (f) Mendlik, M. T.; Cottard, M.; Rein, T.; Helquist, P. *Tetrahedron Lett.* **1997**, *38*, 6375−6378. (g) Tanaka, K.; Otsubo, K.; Fuji, K. *Tetrahedron Lett.* **1996**, *37*, 3735−3738. (h) Abiko, A.; Masamune, S. *Tetrahedron Lett.* **1996**, *37*, 1077−1080.

(12) (a) Becke, A. D. *J. Chem. Phys.* **1993**, *98*, 5648−5652. (b) Lee, C.; Yang, W.; Parr, R. G. *Phys. Rev. B* **1988**, *37*, 785−789.

(13) Gaussian 94, Revision D.1; Frisch, M. J.; Trucks, G. W.; Schlegel, H. B.; Gill, P. M. W.; Johnson, B. G.; Robb, M. A.; Cheeseman, J. R.; Keith, T.; Petersson, G. A.; Montgomery, J. A.; Raghavachari, K.; Al-Laham, M. A.; Zakrzewski, V. G.; Ortiz, J. V.; Foresman, J. B.; Cioslowski, J.; Stefanov, B. B.; Nanayakkara, A.; Challacombe, M.; Peng, C. Y.; Ayala, P. Y.; Chen, W.; Wong, M. W.; Andres, J. L.; Replogle, E. S.; Gomperts, R.; Martin, R. L.; Fox, D. J.; Binkley, J. S.; Defrees, D. J.; Baker, J.; Stewart, J. P.; Head-Gordon, M.; Gonzalez, C.; Pople, J. A. Gaussian, Inc., Pittsburgh, PA, 1995.

Table 1. Energies of the Global Minima of Each Stationary Point along the Reaction Path

	energy relative to **1** + **2a** (kJ/mol)						
computational level	TS1	**3**	TS2	**4a**	TS3	**5**	**6** + **7**
HF/6-31+G*//HF/3-21+G*		22.0		19.9		−82.1	−165.8
HF/6-31+G*		16.2		16.2		−82.7	−161.4
B3LYP/6-31+G*//HF/6-31+G*		−7.1		−14.2		−91.3	−145.7
B3LYP/6-31+G*	−5.4	−8.0	2.5	−15.8	−15.7	*a*	−146.0
MP2/6-311+G**//B3LYP/6-31+G*	−10.4	−21.1	−17.9	−36.8	−36.1		
B3LYP/6-311+G**//B3LYP/6-31+G*	−0.5	−2.6	8.4	−4.9	−4.4		−139.0
+ΔZPE[b]	10.9	12.2	23.5	12.7	13.6		−129.5

[a] Not a stationary point at B3LYP/6-31+G*. [b] ZPE corrections calculated at B3LYP/6-31+G*.

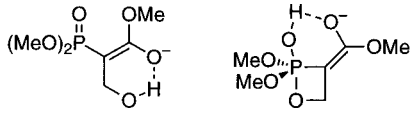

8 **9**

Stationary points on the main reaction path were fully characterized by normal-mode analysis. ZPE corrections were calculated without scaling of the Hessian.[14] At selected points, the energy was calculated at the B3LYP/6-311+G** and MP2/6-311+G** levels of theory.[15] Solvation effects were estimated for the gas-phase geometries using the continuum solvation method PCM/DIR.[16] To evaluate the steric influences on the (*E*)/(*Z*)-selectivity of the reaction, transition states were also located for reactions with acetic aldehyde (**1**; R = Me).

The model system was chosen to reflect reactions in aprotic, low polarity solvents with a noncoordinating counterion.[11e,f,17] The effect of more polar or protic solvent was estimated by single point calculations using PCM/DIR with the B3LYP/6-31+G* wave function. Modern continuum solvation models, including not only electrostatic but also, for example, cavitation effects, generally yield accurate results for the free energy of solvation.[18] In the current study the geometries could not be relaxed with solvation. As relaxation must lower the energy, absolute solvation energies will be *underestimated*. In a relative sense, the effect should be more pronounced when the PES is flatter, as it generally is close to a transition state. A second concern comes from the fact that in a transition state, the surrounding solvent does not have time to reach equilibrium. As the continuum model is parametrized to reproduce the full solvation by a completely equilibrated surrounding, the calculated solvation for the transition state should be *overestimated*. The solvated calculations are useful for predicting trends and isodesmic differences, but absolute values should be treated with care.

Results

Gas-Phase Potential Energy Surface (PES). The energies (relative to the starting materials) of intermediates and transition states calculated at different levels of theory are shown in Table 1.

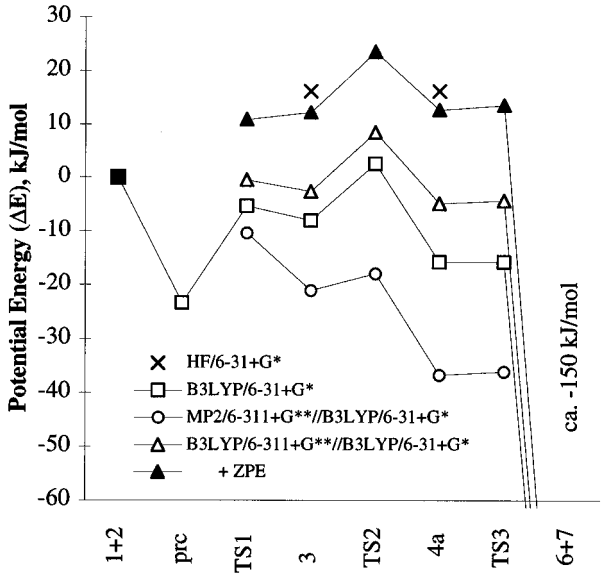

Figure 2. Gas-phase reaction profiles at different levels of theory by using geometries and ZPE corrections from B3LYP/6-31+G*.

The reaction path in Figure 2 shows some variation with theoretical level. It is clear that it is necessary to include electron correlation even in the description of the intermediates. Møller−Plesset (MP2) calculations are fairly reliable, but tend to overcorrect the errors of the Hartree−Fock (HF) solution. The B3LYP hybrid functional is known to give very accurate total energies for a wide range of systems and is generally superior to MP2 in this respect.[15] The B3LYP results will be used in this work, but the discrepancy with MP2 results shows that the relative energies might have an uncertainty around 10−20 kJ/mol.

The most prominent feature of the energy profiles in Figure 2 is that the reaction has a very low energy barrier. The entire profile is also very flat. The total span in energy over all stationary points up to the dissociation of the oxaphosphetane (**1** + **2** → TS3) is less than 20 kJ/mol.

As can be seen in Figure 2, the ZPE contributions have noticeable consequences for the energy profile of the reaction. It is noteworthy that ***3*** *is no longer a minimum*. Even though **3** is a minimum on the potential energy surface of the reaction, the lowest vibrational level is higher than the barrier to dissociation. Thus, the lifetime of **3** in the gas phase is of the same order as one molecular vibration, and the structures should only be viewed as transient. The only transition state of consequence in the gas-phase reaction is the ring closure to oxaphosphe-

(14) The recommended scaling factors for determination of ZPE and thermodynamic vibrational contributions at the B3LYP/6-31G* level are very close to unity: Scott, A. P.; Radom, L. *J. Phys. Chem.* **1996**, *100*, 16502−16513.

(15) B3LYP frequently gives an accuracy equal to or higher than MP2, both for ground and transition state properties: (a) Foresman, J. B.; Frisch, Æ. *Exploring Chemistry with Electronic Structure Methods*, 2nd ed.; Gaussian, Inc.: Pittsburgh, 1996. (b) Frisch, M. J. Presentation at the 213th ACS National Meeting, San Fransisco, 1997. (c) Singleton, D. A.; Merrigan, S. R.; Liu, J.; Houk, K. N. *J. Am. Chem. Soc.* **1997**, *119*, 3385−3386.

(16) PCM/DIR version 2.0, courtesy of Dr. Maurizio Cossi: Cossi, M.; Barone, V.; Cammi, R.; Tomasi, J. *Chem. Phys. Lett.* **1996**, *255*, 327−335.

(17) (a) Rein, T.; Kreuder, R.; Von Zezschwitz, P.; Wulff, C.; Reiser, O. *Angew. Chem., Int. Ed. Engl.* **1995**, *34*, 1023−1025. (b) Rein, T.; Anvelt, J.; Soone, A.; Kreuder, R.; Wulff, C.; Reiser, O. *Tetrahedron Lett.* **1995**, *36*, 2303−2306. (c) Rein, T.; Kann, N.; Kreuder, R.; Gangloff, B.; Reiser, O. *Angew. Chem., Int. Ed. Engl.* **1994**, *33*, 556−558. (d) Kann, N.; Rein, T. *J. Org. Chem.* **1993**, *58*, 3802−3804.

(18) (a) Tomasi, J.; Persico, M. *Chem. Rev. (Washington, D.C.)* **1994**, *94*, 2027−2094. (b) Cramer, C. J.; Truhlar, D. G. In *Reviews in Computational Chemistry*; Lipkowitz, K. B., Boyd, D. B., Eds.; VCH: New York, 1995; Vol. 6, pp 1−72.

Table 2. Estimated Energies in Various Solvents, Relative to the Starting Materials[a]

	energy relative to **1** + **2a** (kJ/mol)					
medium	TS1	**3**	TS2	**4a**	TS3	**6** + **7**
gas phase	12	12	27	13	14	−130
toluene	4	−7	6	−8	−5	−159
diethyl ether	19	4	16	5	7	−173
tetrahydrofuran	−10	−30	−23	−34	−29	−169
dichloromethane	14	−4	5	−5	−2	−169
ethanol	16	−7	11	−5	−2	−171

[a] Potential energies from B3LYP/6-311+G**//B3LYP/6-31+G*. ZPE contributions calculated at B3LYP/6-31+G*. Solvation contributions calculated using PCM/DIR[16] (B3LYP/6-31+G*) at 298K. Values from one representative set of conformers.

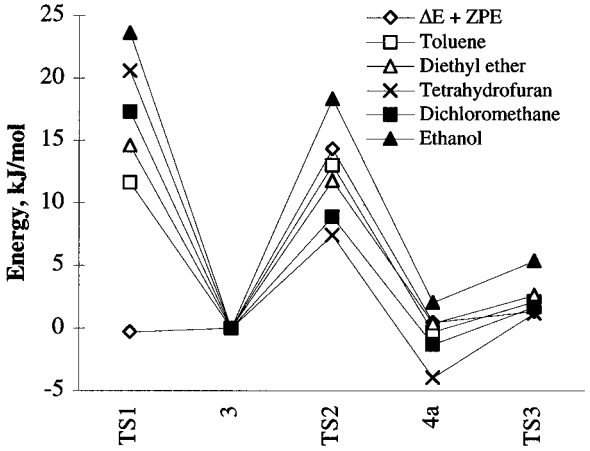

Figure 3. Effects of solvation on the reversibility of the first addition step (kJ/mol). Energies from B3LYP/6-311+G**//B3LYP/6-31+G*, with ZPE contributions and PCM/DIR solvation calculated at B3LYP/6-31+G*.

tane **4** (TS2). It should be noted that according to the MP2 calculations **3** is a true minimum, and TS1 is rate limiting. However, the change in relative energy of TS1 and TS2 is only ca. 16 kJ/mol. This difference is negligible compared to the effects of solvation and steric interactions in real systems.

Solvation. It is clear from the data in Table 1 that the rate-determining step on the B3LYP gas-phase PES is TS2. Further reaction of **4a** is strongly exothermic, with a small activation barrier. However, even in the absence of a counterion, the points on the reaction path leading up to **4** are expected to experience different degrees of stabilization from the reaction medium. For anionic species in particular, the stabilization by solvent will be strongly dependent on the degree of delocalization of the charge. We have therefore attempted to quantify the effect of various solvents by single point calculations using the polarizable continuum model (PCM/DIR) developed by Tomasi and co-workers.[16] The calculated energies (including solvation effects and ZPE) are shown in Table 2, and depicted in Figure 3. It is clear that in solvent, oxyanion **3** is again a true intermediate. Furthermore, in some solvents, TS1 exceeds TS2 in energy even on the B3LYP PES.

Discussion

One of the more interesting aspects of the current study from a computational viewpoint is the change in reaction profile upon solvation. In particular TS1, which could not even be considered a true transition state in the gas phase, has increased in energy relative to other species. In most solvents, TS1 is the rate-determining step. The difference between TS1 and TS2 is likely to be within the limits of uncertainty of the methods employed, but will be more pronounced if the substituents on phosphorus are chosen to stabilize pentacoordination.[9f,h]

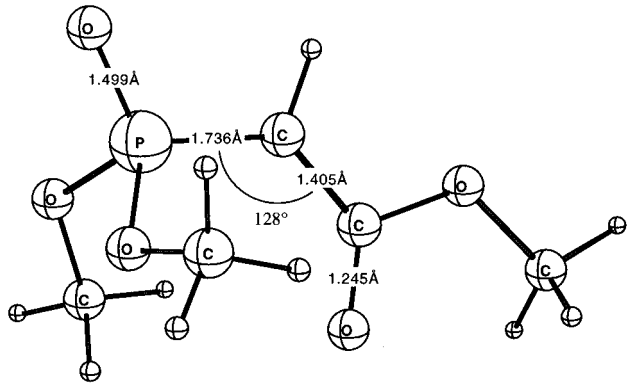

Figure 4. The global minimum of the phosphonate anion at the B3LYP/6-31+G* level (note the large P−C−C angle).

We will now look more closely on each intermediate, and then return to a more detailed discussion of the transition states.

The Phosphonate Reagent 2. The global minimum of **2** in gas phase is shown in Figure 4. The (*E*)-configuration[19] was shown to be more stable than the best (*Z*)-configuration by only 3 kJ/mol. With the PCM solvation model to simulate the presence of THF, the energy difference increased to 12 kJ/mol in favor of the (*E*)-isomer. The barrier to isomerization of the enolate C−C bond was found to be high (ΔE[B3LYP/6-31+G*] = 93 kJ/mol). Thus, the phosphonate anion could be expected to isomerize only slowly at 200 K.[20]

The Oxyanion 3. Oxyanion **3** was found to be computationally unstable, especially in the initial phase using semiempirical calculations. In the gauche form, the aldehyde moiety was found to be only weakly bonded, with a calculated C−C bond length of 1.67 Å at the B3LYP/6-31+G* level (1.60 Å at HF/6-31+G*). The anti form of **3** was found to be a nonstationary point on the B3LYP PES.

Due to the fragmentation of *anti*-**3** in the B3LYP calculations, the relative energies of *gauche*- and *anti*-**3** could only be studied at the HF/6-31+G* PES. Here, the best anti form was found to be 13 kJ/mol higher in energy than the global minimum. Single point PCM/B3LYP/6-31+G* at the HF geometries indicated that *anti*-**3** is more efficiently stabilized by solvation than *gauche*-**3**. In a protic solvent like ethanol, *anti*-**3** was favored by 15 kJ/mol (counting just the solvation contribution, not the vibrational component). These results indicate that *anti*-**3** could be a stationary point on the *solvated* B3LYP PES. Unfortunately the PCM implementation available to us does not allow solvated geometry optimizations. Increasing the bond length of the forming C−C bond by 0.1 Å, followed by relaxation of the remaining degrees of freedom at HF/6-31+G* and single point calculations

(19) Formally, the oxygen priorities may vary with the metal cation. For consistency, in the current work the anionic enolate oxygen is always considered to have a lower priority than the methoxy group.

(20) Bottin-Strzalko, T.; Corset, J.; Froment, F.; Pouet, M.-J.; Seyden-Penne, J.; Simmonin, M.-P. *J. Org. Chem.* **1980**, *45*, 1270−1276.

Table 3. Energies of Conformations of 3 Relative to *gauche*-3[a]

single point level	TS (*gauche*-**3** → *anti*-**3**) $\Delta E^{\ddagger}$ (kJ/mol)	*anti*-**3** ΔE (kJ/mol)
B3LYP/6-31+G*	31	16
$+\Delta\Delta G_{solv}$(toluene)	21	3
$+\Delta\Delta G_{solv}$(diethyl ether)	16	−4
$+\Delta\Delta G_{solv}$(tetrahydrofuran)	17	0
$+\Delta\Delta G_{solv}$(dichloromethane)	13	−11
$+\Delta\Delta G_{solv}$(ethanol)	11	−15

[a] HF/6-31+G* geometries, solvation using PCM/B3LYP/6-31+G* at 298 K, no vibrational contributions included.

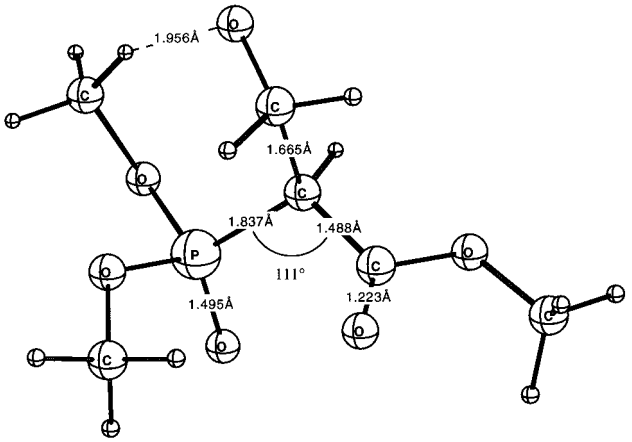

Figure 5. The global minimum of the oxyanion (B3LYP/6-31+G*).

using PCM/B3LYP/6-31+G*, yields an energy increase and confirms that there is a potential energy barrier to fragmentation of *anti*-**3** at the solvated B3LYP PES.

For *anti*-**3** to be on the reaction path, there are two requirements. First, the barrier to formation of *anti*-**3** must be very low (which is confirmed by the current results). Second, there must be a path for conversion of *anti*-**3** to *gauche*-**3**, to enable subsequent P−O bond formation. The conversion of *anti*-**3** to *gauche*-**3** is a simple rotation around a C−C single bond, which is expected to be facile. However, the crowding in the rotation transition state must definitely be worse than in the ground states. As the C−C bond was too weak to allow optimization even of *anti*-**3**, it was not possible to find a gas-phase rotation barrier at the B3LYP level. To elucidate whether *anti*-**3** can be on the reaction path of a solvated system, the two forms of **3** and the interconnecting rotation barrier were investigated on the HF/6-31+G* PES, with subsequent PCM/B3LYP/6-31+G* solvation calculations. The results are shown in Table 3. In the gas phase, the rotation barrier is definitely high enough to preclude any reaction through *anti*-**3** (the rate-determining TS2 is only 15 kJ/mol higher in energy than **3**; Table 2). However, both the rotation barrier and the anti form of **3** are preferentially stabilized by solvation. Although the effect is small, there is a clear trend that more polar solvents will increase the importance of the anti form of oxyanion **3**.

In the global minimum of *gauche*-**3** (Figure 5), the distance between the anionic oxygen and one of the methyl hydrogens is short (1.96 Å), indicating a hydrogen bond interaction. This interaction is not possible for the anti conformers and could therefore be responsible for the large difference in energy and stability between anti and gauche conformers, and also for the difference in solvation.

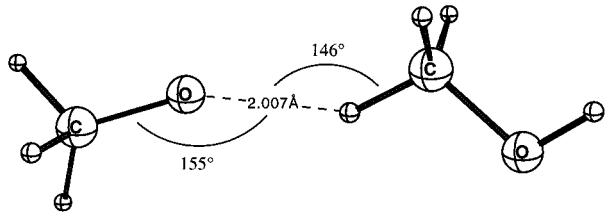

Figure 6. Model system used to evaluate the hydrogen bonding in oxyanion **3**. Geometry from B3LYP/6-311+G(d,p).

It is not a priori certain that the C−H···O stabilization represents a physical situation, especially not for the simple alkyl phosphonates. Quantum chemical descriptions of hydrogen bonding are notoriously sensitive to the level of theory employed.[21] On the other hand, weak interactions between oxygen and activated C−H bonds are frequently observed in the solid state.[22] Also, a partial basis set saturation using single point calculations at the B3LYP/6-311+G** level did not lower the interaction energy noticeably. Therefore, it was decided to investigate this specific interaction using higher levels of theory for a smaller model system (methoxide coordination to the α-protons in methanol). One of the key questions to be answered by the small model study was to estimate the systematic error, if any, in the relative energies of gauche and anti conformers of oxyanion **3**. It was also noted that one of the synthetically most interesting classes of phosphonate reagents, the 2,2,2-trifluoroethyl (TFE) phosphonates,[9c] should be expected to be much stronger hydrogen bond donors than simple alkyl phosphonates. This effect could also be expected in reactions with aryl phosphonates.[9a,b] To evaluate this point, a similar model study was also performed on the coordination of methoxide to the α-protons in 2,2,2-trifluoroethanol.

Modeling the Hydrogen Bonding Situation in Oxyanion 3. The truncated model system used in the calculations is shown in Figure 6. The methoxy group was coordinated to the α-hydrogen trans to the O−H to avoid interference from the alcoholic proton. Optimizing the dimer at B3LYP/6-31+G* resulted in a hydrogen bonding potential energy of 25 kJ/mol.[23] The O−H distance in the dimer is 2.034 Å, very similar to the value in the gauche conformers of the oxyanions. B3LYP single point calculations using the 6-311+G** and 6-311+G-(2d,2p) basis sets gave bonding energies of 27 and 26 kJ/mol, respectively, showing a nice convergence. Counterpoise correction indicated minor basis set superposition errors (−0.8 kJ/mol). Optimizing the geometries at 6-311+G** gave no significant change in energy and an O−H distance of 2.007 Å. Thus, the basis set seems sufficiently saturated for this type of problem already at 6-31+G*, indicating that the gauche stabilization is a real gas-phase effect, not a method artifact. Recent results from a DFT study of hydrogen bonded systems indicate

(21) (a) For a review, see: Scheiner, S. In *Reviews in Computational Chemistry*; Lipkowitz, K. B., Boyd, D. B., Eds.; VCH: New York, 1991; Vol. 2, pp 165−218. (b) For applications of DFT to hydrogen bonded systems, see: Lundell, J.; Latajka, Z. *J. Phys. Chem.* **1997**, *101*, 5004−5009.

(22) For a review, see: Steiner, T. *Chem. Commun.* **1997**, 727−734.

(23) All energies of the methoxide−alcohol dimers in this section include zero-point correction at B3LYP/6-31+G*.

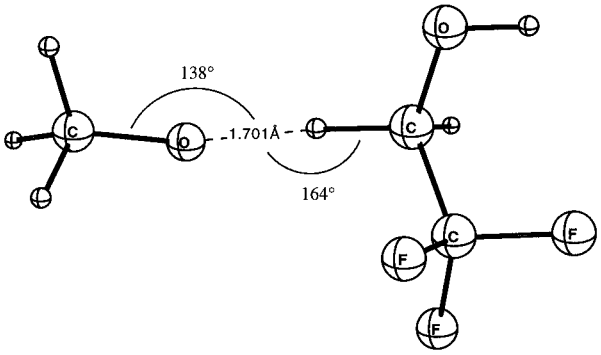

Figure 7. Model system used to evaluate the hydrogen bonding in oxyanions derived from TFE phosphonates. Geometry from B3LYP/6-311+G**.

that hybrid functionals are more reliable than MP2 for this type of problem.[21b]

Single point calculations using the PCM solvation model indicate that in all solvents tested, the complex is disfavored (see Supporting Information), that is, the separated monomers are much more strongly solvated than the complex is. In the real oxyanion *gauche*-**3**, the solvation upon separation cannot be as efficient as in the truncated model system, but the conclusion must still be that for common alkyl phosphonates in a solvent, the effect of the C−H hydrogen bond is minor.

Modeling the Hydrogen Bonding Situation in TFE Reagents. Although it is not very likely that the solvated oxyanion **3** derived from trimethylphosphonoacetate anion should have any gauche preference due to C−H hydrogen bonds, the effect may be more pronounced for stronger C−H donors. TFE reagents are generally highly (*Z*)-selective in their formation of alkene products.[9c] The hydrogens of the TFE groups are considerably more positive than those of methoxy groups.[24] This indicates that TFE groups could form strong hydrogen bonds to anions. To evaluate this possibility, calculations were done on a model system composed of a methoxide anion and a trifluoroethanol molecule (Figure 7). As in the methoxide−methanol system, the alcohol O−H-proton was oriented away from the anion and the dimer was minimized at B3LYP/6-311+G**. In this case the distance between the anionic oxygen and the hydrogen of the TFE was 1.70 Å, and the bonding energy turned out to be about 71 kJ/mol.

Calculations using the PCM solvation model indicated that the separated monomers are more strongly solvated than the complex, as for the methoxide−methanol complex (see Supporting Information). In most solvents, the complex formation is thus disfavored, but in toluene the dimer has a lower energy than the separated monomers.

The model calculations indicate that the C−H···O hydrogen bonding in *gauche*-**3** is a real effect, not a method artifact. The crossover point where *anti*-**3** becomes important cannot be exactly predicted from the current level of theory, but direct formation of *gauche*-**3** should be dominant in any system where unusually strong hydrogen bonds can be formed (e.g., with TFE reagents), and possibly in solvents of low polarity even with regular alkyl phosphonates.

(24) The hydrogen trans to the OH hydrogen has a positive charge of 0.03 in methanol and 0.12 in TFE. The charges were calculated by CHelpG in Gaussian.

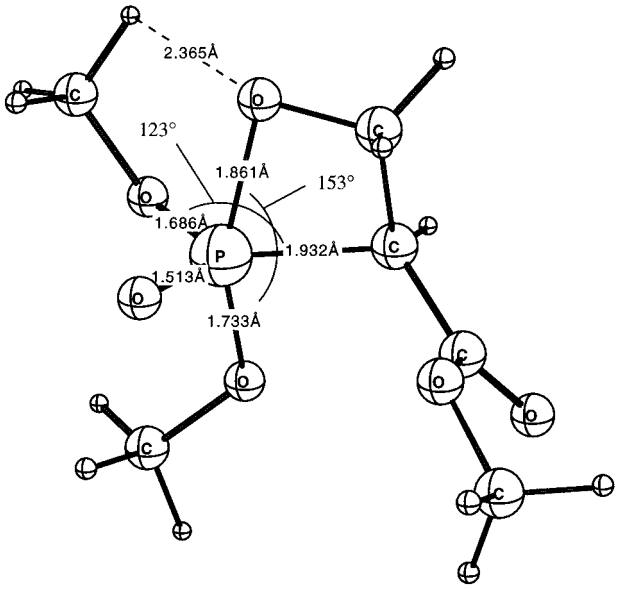

Figure 8. B3LYP/6-31+G* geometry of oxaphosphetane **4a**.

The Oxaphosphetanes 4a and 4b. Computationally, oxaphosphetane **4a** proved to be a rather labile intermediate, easily decomposing into the final products. This is also evident from the frequency calculation at B3LYP/6-31+G*, where the lowest vibrational eigenmode corresponds to pseudorotation.

The configurational preference of five-coordinated phosphorus is well-known, and the current system follows the general rules.[25] The anionic oxygen is apicophobic, that is, it does not go to an apical position. Pseudorotations therefore take place using this oxygen as a pivot. Addition to tetrahedral phosphorus takes place at one face of the tetrahedron, with the attacking group and the atom trans to the reacting face ending up in the apical positions. A direct corollary is that the oxygen attack leading to the formation of an oxaphosphetane can only take place between the oxo substituent and one of the alkoxy groups, not trans to the oxo (vide infra). The geometry of the optimized oxaphosphetane **4a** is shown in Figure 8.

The pseudorotamer **4b** was found to be a nonstationary point on the B3LYP PES. However, it can safely be concluded from the HF/3-21+G$^{(*)}$//AM1 data that although the oxaphosphetane pseudorotamer **4b** is not a stationary point even on the HF/3-21+G$^{(*)}$ PES, it is still very low in energy and very probably part of the reaction path. Any event on the reaction path after formation of **4a** will be unable to influence the rate of the reaction. Influences on the reaction selectivity, on the other hand, are possible, but only if subsequent isomeric intermediates can interconvert (e.g., via C−C bond rotation in **5**, vide infra).

The Enolate 5. HF/6-31+G* calculations yielded a long O−C distance, indicating a rather weak bond (Figure 9). The situation is similar to the case of the oxyanion **3**, where the C−C bond is elongated. In the final calculations using B3LYP/6-31+G*, the potential intermediate **5** optimized to give the final products. It is consequently reasonable to assume that this intermediate, if it exists in real reactions, is very short-lived, and

(25) Gillespie, P.; Ramirez, F.; Ugi, I.; Marquarding, D. *Angew. Chem., Int. Ed. Engl.* **1973**, *12*, 91−126.

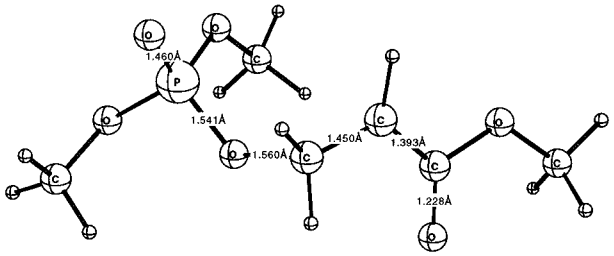

Figure 9. The geometry of the optimized ring-opened enolate **5** (HF/6-31+G*).

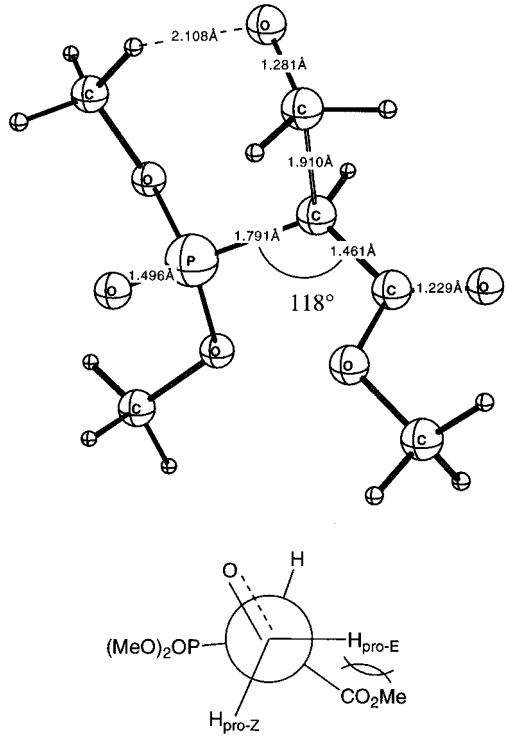

Figure 10. The lowest transition state found leading to the oxyanion **3** (TS1, B3LYP/6-31+G*). Note the large P−C−C angle in the phosphonate reagent, leading to unexpected steric crowding with the pro-(*E*) aldehyde substituent.

the possibility for isomerization via crossover between diastereomeric pathways through C−C bond rotation is small. The elimination will be even more favored by electron-withdrawing substituents on phosphorus (e.g., as in TFE reagents). It should be noted, however, that solvation generally disfavors dissociation (due to the positive activation volume). An isomerization path leading to an enrichment of (*E*)-isomer cannot be completely excluded in anion-stabilizing media.

The Addition Transition State, 1 + 2 → *gauche*-3 (TS1). Two different transition states have been identified, corresponding to the two lowest energy conformers of the oxyanion *gauche*-**3**. The two transition states mainly differ in rotation around the C−P bond. The lowest energy form of TS1 is shown in Figure 10.

The transition state is late, showing large similarities to oxyanion **3**. There is an interaction between the aldehyde oxygen and a hydrogen from the methoxy group already in the transition state (similar to that found in the oxyanion *gauche*-**3**), a factor which could be of importance in the case of TFE- or phenyl-based phosphonate reagents, but probably not when employing common alkyl phosphonates (*vide supra*). There is also

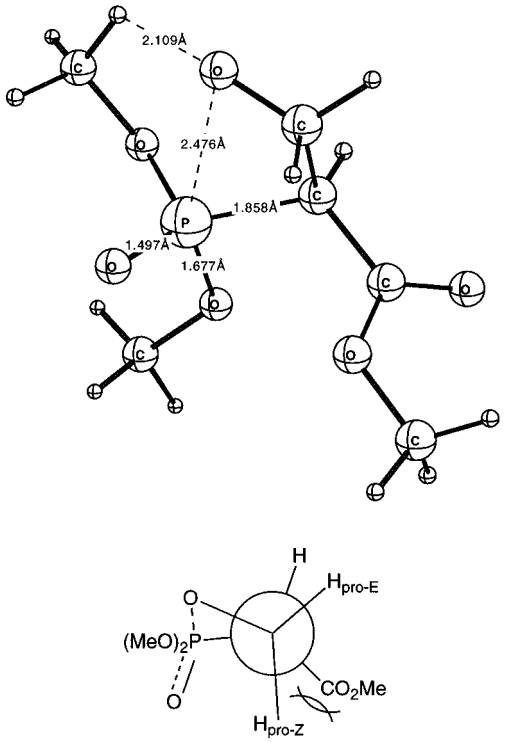

Figure 11. The transition state leading to the oxaphosphetane **4a** (TS2, B3LYP/6-31+G*).

a close steric interaction between the ester group and the pro-(*E*) formaldehyde proton. The C−C−C−$H_{pro-(E)}$ dihedral angle is only 28−35° in the two characterized transition states. This somewhat surprising result is counter-intuitive and shows that the Newman projection in Figure 1 represents an oversimplification. Due to the large angle between the phosphonate and ester in reagent **2** (Figure 4, *vide supra*), the least hindered position for the aldehyde group in TS1 may actually lie between the two large groups, leading to a predicted (*Z*)-selectivity from the gauche-addition transition state.

The steric crowding of pro-(*E*)-substituents in TS1 is a result of the torsion around the forming C−C bond, and thus indirectly of the hydrogen bond between the phosphonate C−H and the forming oxyanion. Without the additional rigidity imposed by this hydrogen bond, a pro-(*E*) substituent might be accommodated by a slight rotation around the forming bond.

No transition state in which the aldehyde oxygen is located gauche to both the ester and the phosphonate group (*gauche*-g-TS1, Figure 1; *vide supra*) was characterized, since the corresponding conformers of the oxyanion **3** were at least 12 kJ/mol higher in energy than the global minimum.

The Ring Closure Transition State, 3 → 4a (TS2). A detailed look at the transition state structure (Figure 11) reveals that the forming four-membered ring is less planar than might have been expected intuitively. The eclipsing between the ester group and the pro-(*Z*) hydrogen is not fully developed. The C−C−C−H_{pro-Z} dihedral angle is 43° in the transition state, not 0° as would be expected in a completely planar ring. However, the vibrational analysis reveals that the reaction coordinate contains a large C−C bond rotation component, which will lead to an even stronger disfavoring of the pro-(*Z*)-TS2.

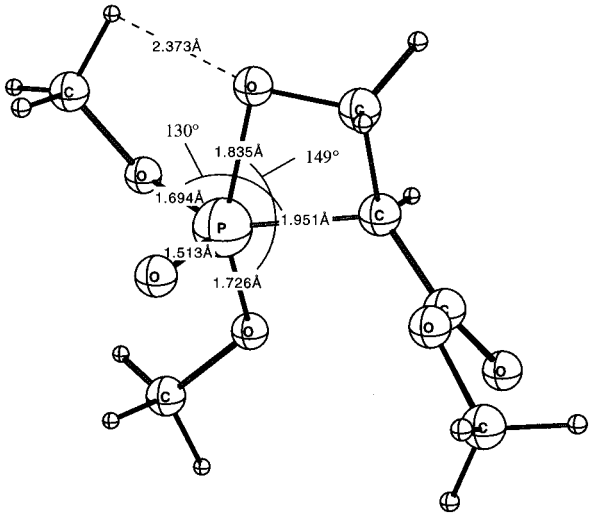

Figure 12. The transition state for the decomposition of oxaphosphetane **4a** (TS3, B3LYP/6-31+G*).

The hydrogen bond donation from C−H to the anionic oxygen is still observed in the gas-phase TS2, but no longer has any significant effect on the transition state geometry, as the charge on oxygen has been lowered by interaction with phosphorus. The general conclusion is that TS2 will favor (*E*)-product formation.

A transition state originating from the conformation of the oxyanion shown in Figure 5, where the oxo oxygen on phosphorus is in an anti orientation to the attacking oxygen, was also evaluated. This turned out to be 37 kJ/mol higher in energy and should therefore not be located on the reaction pathway.

The Transition State between 4a and the Final Products (TS3). Pseudorotation from **4a** takes place using the anionic oxygen ligand on phosphorus as a pivot, forming **4b** as a nonstationary point on the reaction PES. The transition state for this reaction step has been located, using B3LYP/6-31+G*, to be very close to **4a** as could be expected from Hammond's postulate, and it is structurally very similar to **4a** (Figure 12). The barrier was found to be negligible in the gas phase.

Origin of Geometric Selectivities. As mentioned eartlier, a rate-determining TS2 should always result in an overall (*E*)-selectivity of the reaction. To achieve (*Z*)-selectivity it is necessary to use conditions stabilizing TS2, but also to disfavor (*E*)-selective forms of TS1. An irreversible addition through *anti*-TS1 (Figure 1) is one possible way of rationalizing (*Z*)-selective HWE reactions. According to the calculations, the (*Z*)-selective route via *anti*-TS1 should be of increased importance in dichloromethane or ethanol and of less importance in THF or toluene.

Two additional scenarios can be envisioned, both of which can explain the shift toward (*Z*)-selectivity when TFE or aryl phosphonates are employed. Either *gauche*-a-TS1 could be (*E*)-selective with ordinary alkyl phosphonates but (*Z*)-selective with reagents that can form a C−H hydrogen bond, or alternatively *gauche*-a-TS1 is always (*Z*)-selective and the shift in geometric selectivity is due to a shift in rate determining step from TS2 to TS1 when **4a** is stabilized. To investigate these points, calculations were performed on diastereomeric forms of *gauche*-TS1 in reactions of acetaldehyde with trimethyl phosphonoacetate (**2**) as well as with a model for a TFE-based phosphonate reagent (**10**, see Figure 13). In reagent **10**, the hydrogen bonding methoxy group has been replaced with a 2,2,2-trifluoroethoxy group.

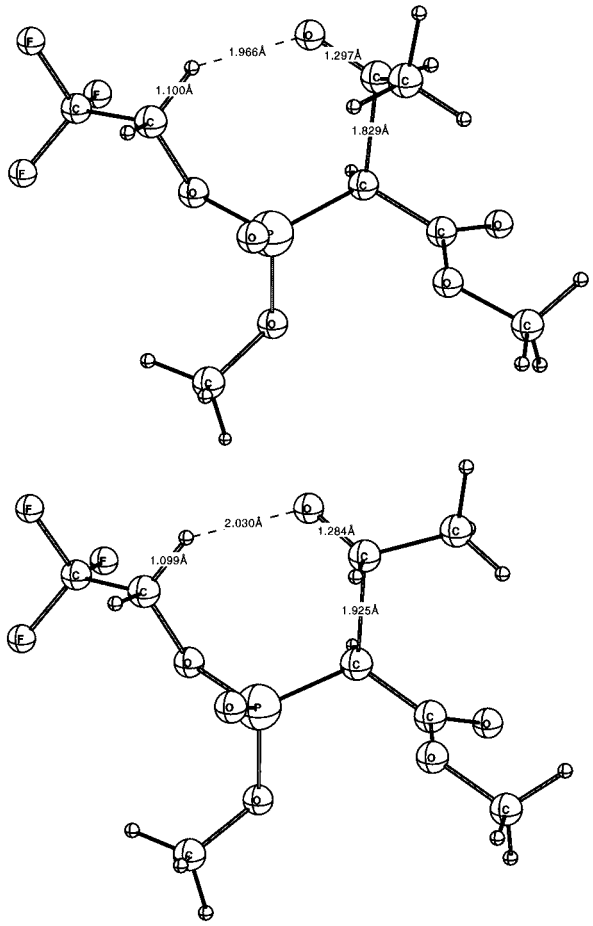

Figure 13. A comparison of pro-(*Z*) (top) and pro-(*E*) (bottom) forms of *gauche*-TS1 in the reaction of acetaldehyde with phosphonate **10**. The pro-(*Z*) isomer shows a more strongly developed hydrogen bond.

The results from these calculations indicate that the TFE-based reagent does indeed shift the selectivity toward (*Z*)-product compared to **2** (see Supporting Information). The selective favoring of pro-(*Z*) TS1 when employing ligands with active hydrogens emerges from this transition state being later compared to pro-(*E*) TS1 (see Figure 13). A later TS1 will have a more developed anionic character on the aldehyde oxygen and thus will gain more by a hydrogen bond stabilization.

Examining the results from the diaryl phosphonoacetates introduced recently,[9a,b] the (*Z*)-selectivity observed could be rationalized as resulting from C−H hydrogen bonding. It is striking that exchanging both of the potential hydrogen bond donor hydrogens in the ortho positions decreases the (*Z*)-selectivity.[26] Furthermore, the higher (*Z*)-selectivity obtained with reagents containing electron-withdrawing aryl substituents could result from increased C−H hydrogen bonding.

Stabilization of pentacoordinate phosphorus by employing cyclic phosphonates leads to increased levels of (*Z*)-selectivity.[9f,g] Since C−H hydrogen bonding is unlikely in this case, this indicates that *anti*-TS1 is of importance with these reagents.

(26) The decreased (*Z*)-selectivity could alternatively be due to increased steric interactions in TS2.

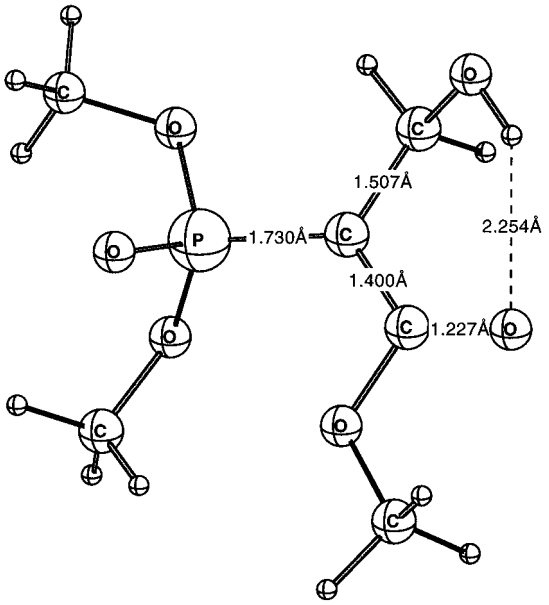

Figure 14. Geometry of the hydroxy-enolate **8** (HF/6-31+G*).

Epimerization of 3 and 4a. Diastereomeric Crossover. To evaluate the possibility of tautomerization of intermediates, we have considered the possibility that **3** might have a long enough lifetime to enable proton transfer from the α-carbon, yielding hydroxy-enolate **8** (Figure 14). Proton transfer in **3** can affect the overall reaction selectivity only under certain conditions. In the case where **3** is formed reversibly, with an overall rate determining TS2, the side path can have *no* effect on the final reaction selectivity. If, on the other hand, reaction conditions are such that TS1 becomes rate determining, scrambling at the α-carbon would have the effect that TS2 again becomes *selectivity* determining, with a final product distribution of the same type as the one obtained with a rate-determining TS2. At the B3LYP/6-31+G*//HF/6-31+G* level, **8** is indeed a stationary point, at an energy level 54 kJ/mol lower in energy than **3**, and should probably have about the same free energy as the reactants. Thus, tautomerization of **3** could influence the final product selectivity if the barrier for tautomerization is lower than TS2.[4b,7] We note that intermediates of type **8** have been implicated as potential intermediates in apparent addition of a phosphonoacetate reagent to *both* aldehyde moieties in a dialdehyde.[27] However, such bisaddition products could also result from addition of **5** to the second aldehyde moiety.

Despite the strong calculated exothermicity of the further conversion of **4a** to **5**, we also considered the possibility that **4a** might be long-lived enough to allow tautomerization via reversible formation of **9** (Figure 15). At the B3LYP/6-31+G*//HF/6-31+G* level, **9** is 39 kJ/mol higher in energy than **4a**. This result makes epimerization via **9** very improbable, in particular in view of the very low barrier to further conversion of **4a** into the final products.

Further Studies. The current work has been limited to the addition of a naked phosphonate anion to simple aldehydes. The study is relevant to some commonly employed experimental conditions for the HWE reaction. The currently employed levels of calculation cannot possibly be scaled up to systems where asymmetric induction is of interest. To enable evaluation of larger systems, where nonbonded interactions between distant moieties of the complex may have a large influence on the selectivity, we have initiated a molecular mechanics study employing the transition state structures determined herein. We plan to employ a selectivity model based on the current results in a search for even more efficient reagents in asymmetric versions of the HWE reaction.[11]

(27) See ref 1e, page 104.

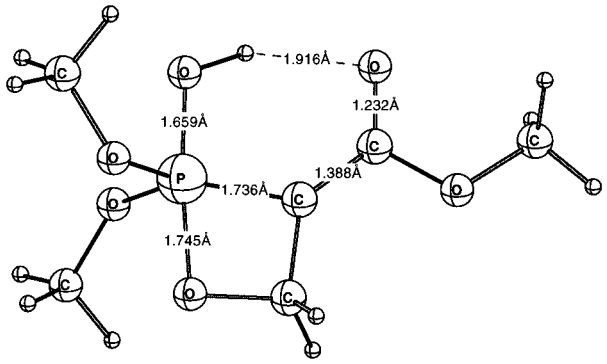

Figure 15. Geometry of the hydroxy-enolate **9** (HF/6-31+G*).

Our results also suggest further experimental studies of the mechanism of the HWE reaction. The transition state structures determined here allow prediction of kinetic isotope effects in the different steps. The predicted isotope effects can then be tested at natural abundance using the methods of Singleton and coworkers.[15c,28] Of special interest would be to find the crossover point in reaction conditions between rate-determining TS1 or TS2. If a crossover point is found to exist, it might also be of interest to search for a nonlinearity in the temperature dependence of the selectivity, according to Scharf et al.[29]

Conclusions

The mechanism of the HWE reaction under noncoordinating reaction conditions has been investigated in the gas phase and with a continuum solvation model. The rate-determining step in gas phase was found to be ring closure of the P−O bond to form an oxaphosphetane (TS2; **3** → **4a**). Oxyanion **3** was not a true intermediate in the gas phase, but with solvation effects included, oxyanion **3** became a minimum on the reaction path. The addition step (TS1; **1** + **2** → **3**) is rate-determining in most solvated systems. TS2 is always expected to favor formation of (*E*)-product, whereas TS1, according to the current results, shifts toward (*Z*)-selectivity when hydrogen bond donor ligands are used on phosphorus. No reaction path leading through an anti addition step (*anti*-TS1) could be located, but could exist in solvated systems. Isomerization side paths did not seem to be important under the currently investigated conditions, but need to be

(28) (a) Singleton, D. A.; Thomas, A. A. *J. Am. Chem. Soc.* **1995**, *117*, 9357−9358. For a recent application, see: (b) Frantz, D. E.; Singleton, D. A.; Snyder, J. P. *J. Am. Chem. Soc.* **1997**, *119*, 3383−3384.

(29) (a) Gypser, A.; Norrby, P.-O. *J. Chem. Soc., Perkin Trans. 2* **1997**, 939−943. (b) Norrby, P.-O.; Gable, K. P. *J. Chem. Soc., Perkin Trans. 2* **1996**, 171−178. (c) Hale, K. J.; Ridd, J. R. *J. Chem. Soc., Perkin Trans. 2* **1995**, 1601−1605. (d) Hale, K. J.; Ridd, J. R. *J. Chem. Soc., Chem. Commun.* **1995**, 357−358. (e) Buschmann, H.; Scharf, H.-D.; Hoffmann, N.; Esser, P. *Angew. Chem., Int. Ed. Engl.* **1991**, *30*, 477−515.

considered under conditions where localized anions are stabilized. Several effects that could rationalize experimentally observed trends for (*E*)/(*Z*)-selectivities have been identified. It is also important to note that the whole path must be considered for any type of selectivity prediction, as selective disfavoring of any transition state on the path could make that transition state rate-determining.

Acknowledgment. Financial support from the Swedish Natural Science Research Council, the Carl Trygger Foundation, Pharmacia&Upjohn, the Ernst Johnson Foundation, the Estonian Science Foundation, and the Danish Medical Research Council is gratefully acknowledged. We are grateful to Professor Jacopo Tomasi and Dr. Maurizio Cossi for a copy of the PCM/DIR program. Access to supercomputer time was provided by the National Supercomputer Centre in Linköping, Sweden, and this work was also supported with computing resources by the Swedish Council for High Performance Computing (HPDR) and Parallelldatorcentrum (PDC), Royal Institute of Technology. We also acknowledge Professor Oliver Reiser, University of Regensburg, and Professor Paul Helquist, University of Notre Dame, for stimulating discussions.

Supporting Information Available: Conformational search data, details concerning the hydrogen bond model system, and Cartesian coordinates of all stationary points (7 pages). This material is contained in libraries on microfiche, immediately follows this article in the microfilm version of the journal, and can be ordered from the ACS; see any current masthead page for ordering instructions.

JO971973T